Colloid Polym Sci 278:169–175 (2000)

ORIGINAL CONTRIBUTION

A. Walter
H. Rehage
H. Leonhard

Shear-induced deformations of polyamide microcapsules

Received: 5 July 1999
Accepted in revised form: 30 August 1999

Presented at the 39th General Meeting of the Kolloid-Gesellschaft Würzburg, 27–30 September 1999

A. Walter (✉) · H. Rehage · H. Leonhard
Institut für Umweltanalytik
Universität Essen, Universitätsstrasse 3-5
D-45141 Essen, Germany
e-mail: anja.walter@uni-essen.de
Tel.: +49-201-1833988
Fax: +49-201-1833951

Abstract The application of microcapsules for technical, cosmetic and pharmaceutical purposes has attracted increased interest in recent years. The design of new capsule types requires a profound knowledge of their mechanical properties. Rheological studies provide interesting information on intrinsic membrane properties and this information can be used to avoid premature release of encapsulated compounds due to the action of external mechanical forces (stirring, swallowing, spreading). In this publication we report a systematic study of polyamide microcapsules. These particles were synthesized by reacting 4-aminomethyl-1,8-diaminooctane and sebacoyl dichloride at the interface between silicone oil and water. Two different experiments were performed to get information on the mechanical properties of the capsule walls. First of all, we used an optical rheometer (rheoscope) to observe the capsule deformation and orientation in shear flow. The polymerization kinetics, relaxation properties, the regime of linear-viscoelastic behavior and the shear modulus of the flat membranes were independently measured in an interfacial rheometer. Both experiments gave complementary results. It turned out that the two-dimensional elongational modulus was about 3–4 times larger than the shear modulus. This result is in fairly good agreement with a theoretical model recently proposed by Barthès-Biesel. Due to the simple synthesis and well-defined structure, polyamide microcapsules can also serve as simple model systems to understand the complicated flow properties of red blood cells.

Key words Microcapsule · Interfacial polymerization · Deformation · Young's modulus · Shear modulus

Introduction

Microcapsules have received increased interest in recent years and are nowadays applied in a wide range of products including food, pharmaceutical, agrochemical and cosmetic formulations [1]. Most of these applications are associated with the controlled release of active ingredients under well-defined conditions. Detailed knowledge of wall properties, such as stability, is essential to design special types of capsules with tailor-made release properties. Mechanical forces induced by swallowing (10^1–10^2 s^{-1}), stirring (10^1–10^3 s^{-1}) or spreading (10^4–10^5 s^{-1}) are often linked to undesired deformation and breaking processes of the capsules [2].

Polyamide microcapsules are ideal model systems on grounds of their simple synthesis and defined structure. Many of these systems have already been extensively studied. Mathiowitz and Cohen [3, 4] analyzed capsules of various amine and acid chloride monomers with respect to their controlled release properties, placing special emphasis on membrane characterization. Janssen and coworkers [5–7] focussed on capsules which were

prepared by interfacial polycondensation of terephthaloyl dichloride and diethylene triamine. These authors developed a simple model for membrane growth and permeability. The mechanism of nylon-6,10 formation was carefully analyzed by Enkelmann and Wegner [8, 9], who studied the basic mechanisms of surface gelations.

All these structural characterizations are important but are not sufficient because microcapsules can show a broad range of different membrane features, ranging from purely viscous to elastic properties. Available methods to measure these phenomena are membrane aspiration [10], capsule-squeezing techniques [11] and the determination of capsule orientation or deformation in shear flow [12]. Another experimental technique consists of observing the particle in a spinning-drop tensiometer [13]. Additional results can be obtained by measuring the rheological properties of the flat membranes using an interfacial rheometer [14]. Each of these measurements gives complementary findings, but in order to get more comprehensive information on the constitutive law of the cross-linked membranes, one has to combine several experimental techniques. In this publication, we focus on two rheological methods: capsule deformation in shear flow and rheological measurements of the flat membranes. The objective is to find new correlations between these independent types of experiments.

Determination of mechanical properties of a single microcapsule in simple shear flow is a field of research which has been treated extensively using different types of theory [15, 16]. Unfortunately there are only very few experiments which can be used to test these theoretical models. Chang and Olbricht [12, 17] were probably the first to confirm the theoretical predictions by means of flow-induced capsule deformation experiments. These authors investigated diethylene triamine/sebacoyl dichloride polyamide capsules. In addition to these experiments investigations were also performed with capsule-squeezing techniques. In order to gain more insight into the mechanical stability of the enclosing membranes, we have focussed on the shear rheological properties of the ultra-thin films. The present studies were performed with chemically cross-linked polyamide flat membranes and microcapsules. These systems were synthesized by interfacial polycondensation of 4-aminomethyl-1,8-diaminooctane and sebacoyl dichloride.

Experimental

Materials

4-Aminomethyl-1,8-diaminooctane (Fluka), sebacoyl dichloride, 97% (Aldrich), silicone oil DC 200 with a viscosity of 964 mPas (Fluka) and anhydrous sodium carbonate p.a. (Fluka) were used as received. Sebacoyl dichloride was stored under an argon atmosphere. Aqueous solutions were prepared using tridistilled water.

Polyamide microcapsules

Preparation

Spherical microcapsules were synthesized following a modification of the interfacial polymerization procedure introduced in Ref. [18]. Special requirements of the optical flow cell regarding the solvent phase had to be taken into account. A solution of 10 mmol/l 4-aminomethyl-1,8-diaminooctane in 10 mmol/l aqueous sodium carbonate was quickly emulsified in silicone oil containing 1 mmol/l sebacoyl dichloride. The solution remained unstirred and the capsules were allowed to sediment slowly. After distinct polymerization times, the capsules were carefully transferred to an optical flow cell which contained pure silicone oil as a solvent phase.

Apparatus

The rheoscope consisted of a flow cell (Fig. 1) which was inserted into an inverse microscope.

The flow cell had Couette geometry: two concentric motor-driven cylinders formed an annular liquid-filled gap. The radii of the cylinders were 42.4 and 41.0 mm. This resulted in a gap width of 1.4 mm. The outer cylinder had glass windows which allowed particles within the annular gap to be observed. Detailed analysis of particle deformation and orientation was performed with a high-speed video camera (Kodak Motion Corder Analyzer SR Ultra). By rotating the cylinders in opposite directions, a linear shear field was induced in the gap. Simple shear flow requires small Reynolds numbers, thus avoiding turbulence. This is achieved by using a highly viscous solvent phase and low rotational speeds of the concentric cylinders. As a response to the shearing forces, the microcapsules tend to deform and align themselves with respect to the streamlines. Records of capsule deformations and data files containing the corresponding shear rates were taken with a maximum frequency of 250 frames per second. The capsule images were digitized and analyzed employing special routines of OPTIMAS 6.0, an image-treatment software.

Flat polyamide membrane

Preparation

A sufficient amount of 10 mmol/l 4-aminomethyl-1,8-diaminooctane in 10 mmol/l aqueous sodium carbonate was poured into the outer cylinder of the Rheometrics spectrometer. The measuring plate was carefully brought into close contact with the water air surface. Special attention was needed to avoid the formation of air bubbles. The aqueous phase was afterwards covered with 30 ml of a fresh solution of 1 mmol/l sebacoyl dichloride solved in highly viscous silicone oil.

Apparatus

The interfacial rheometer (Fig. 2) was based on a conventional Rheometrics Scientific RFS II rotational spectrometer. We developed special measuring tools in order to analyze two-dimensional

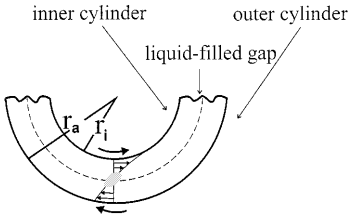

Fig. 1 Schematic drawing of a microcapsule in the flow cell

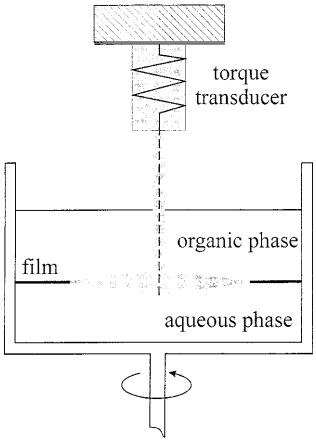

Fig. 2 Sideview schematic drawing of an interfacial rheometer

film properties. The outer cylinder consisted of a glass cup firmly attached to the motor unit. The measuring tool consisted of a biconical titanium plate which was placed exactly at the interface between the oil and the water. All polymerized films adhered to the glass cup and the measuring plate. Measurements and polymerization procedures were always started simultaneously.

The apparatus worked according to the Couette principle: a sinusoidal load was applied to the outer cup and the biconical plate measured the induced torque. From the phase difference between strain and stress and the amplitudes of these functions the two-dimensional storage modulus G' and the loss modulus, G'', could be calculated. Three different types of measurement were carried out: a time-sweep experiment allowing the process of surface gelation to be followed, a frequency-sweep experiment, which gave information on the relaxation properties of the cross-linked structure, and a strain-sweep experiment, which allowed the regime of linear viscoelastic response to be calculated. The last experiment was also performed to gain information on film rupture processes.

Results

Microcapsules

The behavior of a capsule in linear shear flow can be characterized by three experimentally observable parameters [19]:

- The deformation, D, which is defined as the ratio of the major axis length, L, and the minor axis length, B, of the ellipsoidally deformed particle.

$$D = \frac{L - B}{L + B} \tag{1}$$

- The orientation of the capsule in the direction of flow, defined by the angle θ between the principal axis of the microcapsule and the undisturbed streamlines.
- The membrane rotation velocity, ω_T, determined by attaching tracer particles to the surface of the surrounding membrane.

Owing to the experimental setup of the rheoscope, these quantities were all determined within the shear plane.

The behavior of an initially spherical microcapsule in linear shear flow is described by the ratio of deforming and restoring forces. This parameter is often denoted as the capillary number, C.

$$C = \frac{\mu G A}{E_s} \tag{2}$$

Here μ describes the viscous resistance of the solvent phase. G is the applied shear rate and A is the radius of the undeformed capsule. The viscosity ratio of the internal and outer (solvent) phases is usually defined as λ. The constant E_s describes an effective elastic modulus which is composed of two modes of deformation, namely pure shear and area dilatation.

There are some basic restrictions for the following theoretical approach. First of all, the capsule is required to be freely suspended in a Newtonian incompressible liquid with viscosity μ. The particle is filled with an incompressible Newtonian liquid of viscosity $\lambda\mu$ and is surrounded by a three-dimensional volume-incompressible membrane of the Mooney–Rivlin type. Buoyancy effects are neglected and the Reynolds number of the flow based on the capsule dimensions is assumed to be much smaller than unity.

The capsule membrane can display different types of behavior, ranging from purely elastic to viscous properties [20]. In the case of an initially spherical capsule undergoing small deformations ($C \ll 1$) the results can be obtained by a perturbation method. For a purely elastic membrane, D is a linear function of C, which mainly depends on the shear rate. According to the theory of Barthès-Biesel, the orientation angle of the microcapsule remains constant under these conditions.

$$D = \frac{L - B}{L + B} = \frac{25C}{4} + O(C^2) \tag{3}$$

$$\theta = 45^\circ \tag{4}$$

Here, the second term, $O(C^2)$, is much smaller than the first. It denotes a more complicated expression, which can be calculated from the theory of Barthès–Biesel [21]. For a viscoelastic membrane D increases with shear rate, but approaches an asymptotic limit at $D_\infty = C/2\beta = 5\mu A/2\mu_s$, with β referring to the Deborah number and μ_s representing the membrane viscosity. The orientation angle decreases with increasing shear rate from 45° to 0°.

If elastic effects are negligible and the membrane is purely viscous, no steady deformed state is attained, but the membrane continuously inflates and deflates. As a consequence the orientation angle oscillates between −45° and 45°.

Due to the nature of the interfacial polycondensation, the synthesized polyamide membrane is not infinitely thin, but instead has an asymmetric structure with finite thickness. It consists of a smooth primary layer on the aqueous side and a porous secondary layer on the

organic side [5]. Despite knowledge of the existence of a more complicated molecular structure the membrane behavior during flow is just characterized by a single elastic modulus. This constant can be obtained as the product of the bulk Young's modulus, E, and the thickness of the membrane, h, [20].

$$E_s = Eh \tag{5}$$

According to this definition, E_s denotes the two-dimensional elastic modulus.

Equation (3) can now easily be modified

$$D = \frac{25\mu GA}{4Eh} + O(C^2) \tag{6}$$

This difference between the two- and three-dimensional material constants does not affect the analysis of the experimental data.

For all measurements, the Reynolds criterion was carefully examined and linear flow conditions were applied. The viscous resistance of the solvent phase was 0.964 Pas and the viscosity ratio was adjusted to 0.001. The densities of the solvent and the internal phases were almost equal, with the latter being slightly denser. The microcapsule radii varied between 150 and 250 μm and the applied shear rates ranged from 0 to 80 s^{-1}.

The deformation behavior of polyamide microcapsules in linear shear flow is demonstrated in Fig. 3.

These images show a capsule in its quiescent state and under the action of shear forces. The deformed capsule has obtained an ellipsoidal shape and a distinct orientation with respect to the streamlines.

In a series of measurements microcapsules were polymerized for 5–60 min. Typical results of the flow-induced deformation and orientation angles are summarized in Figs. 4 and 5.

Figure 4 shows a linear relationship between deformation and shear rate. From the slope, b, of this line, the elastic modulus can be calculated using the following equation:

$$E_s = Eh = \frac{25\mu A}{4b} \quad . \tag{7}$$

The values determined for different polymerization times are represented in Fig. 9. Figure 4 indicates a slight deviation from linearity for elevated shear rates, but there is no indication of an impending asymptotic deformation limit. This points to the existence of a purely elastic sheet with small viscous contributions.

The broad distribution of deformation values corresponding to one value of the shear rate is caused by a shape oscillation phenomenon.

The shear-induced orientation process of a microcapsule is summarized in Fig. 5. It is easy to see that in the range of the shear rates applied the angle remains nearly constant. This observation supports the elastic wall model, the small decrease can be attributed to

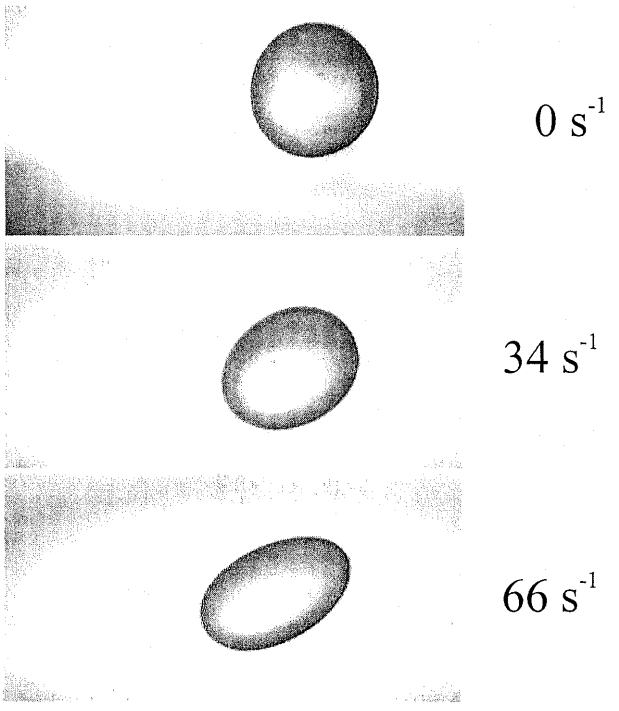

Fig. 3 Photographs of a microcapsule subjected to shear rates of 0, 34 and 66 s^{-1}

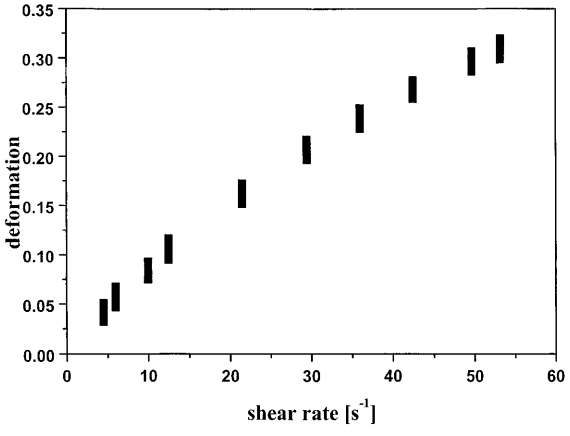

Fig. 4 Capsule deformation as a function of shear rate: t = 20 min; A = 222 μm

$O(C^2)$ effects [20] and marginal viscous properties. The large scattering of orientation angles is again caused by the oscillation phenomenon of the capsules.

The membrane rotation velocity, ω_T, was found to be directly linked to the shape oscillation angular frequency, ω_{osc}

$$\omega_T = \frac{\omega_{osc}}{2} \quad . \tag{8}$$

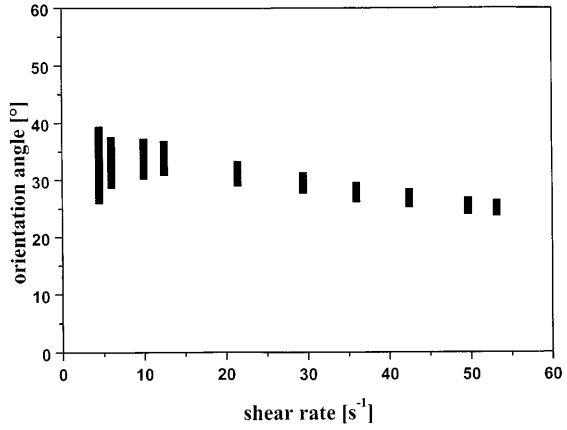

Fig. 5 Orientation of the capsule as a function of shear rate: t = 20 min; A = 222 μm

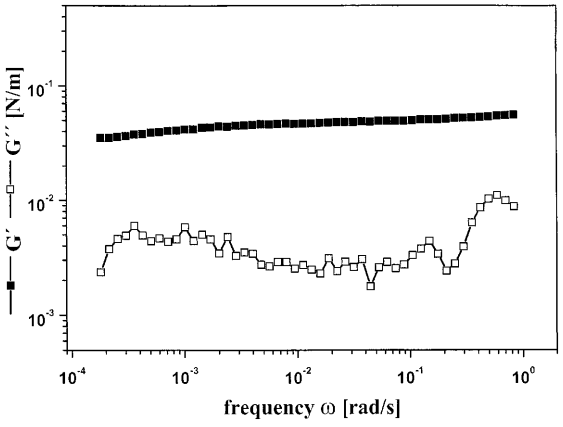

Fig. 7 Frequency-sweep experiment (γ = 0.2%, polymerization time 20 min)

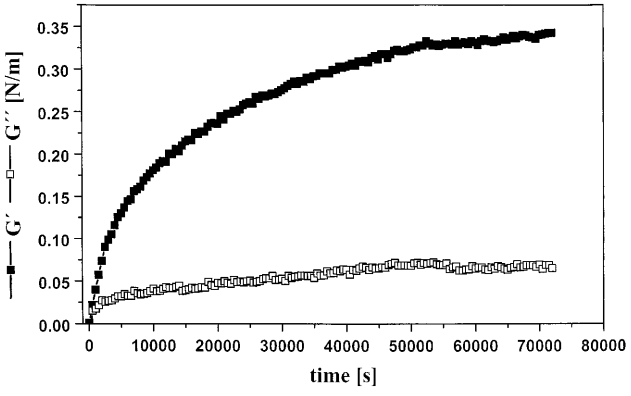

Fig. 6 Time-sweep experiment of a flat membrane (ω = 2 rad/s, γ = 0.2%)

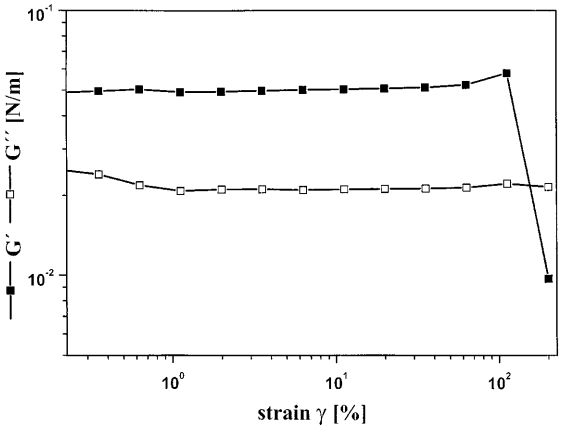

Fig. 8 Strain-sweep experiment (ω = 2 rad/s, polymerization time 20 min)

Flat membrane

The formation of the flat polyamide membrane takes a long time. The cross-linking reactions are terminated as soon as G', has reached a finite plateau value. In the present case, the evolution of G' starts immediately, but the plateau value is reached after a reaction time of about 15 h (Fig. 6).

This contradicts postulations that the reaction is immediately quenched because the newly formed membrane serves as a diffusion barrier. As it is possible to stop the polycondensation reaction by exchanging the solvent at any instant, we can use Fig. 6 to predict the elastic properties of membranes which were only polymerized for finite time intervals. For microcapsules, we used typical polymerization periods of about 20 min. In order to get more information on the relaxation properties of these cross-linked structures, we measured the storage modulus and the loss modulus as a function of the angular frequency. Relevant data are summarized in Fig. 7.

G' turns out to be almost independent of the frequency. This points to the existence of a rubber elastic, cross-linked membrane. It is interesting to note that G'' is about one decade smaller than G'. The viscous properties are, therefore, not so important as the mechanism of energy storage.

The stability of the polyamide membrane polymerized for 20 min can be deduced from Fig. 8.

G' remains constant up to a value of 200% deformation. This is typical for rubber–elastic materials. The decrease in the modulus is due to non-linear effects or it can also be caused by network rupture.

Comparison of the shear modulus of flat membranes and the elongational modulus of microcapsules

In a series of experiments we measured the surface Young's moduli of microcapsules for different polymer-

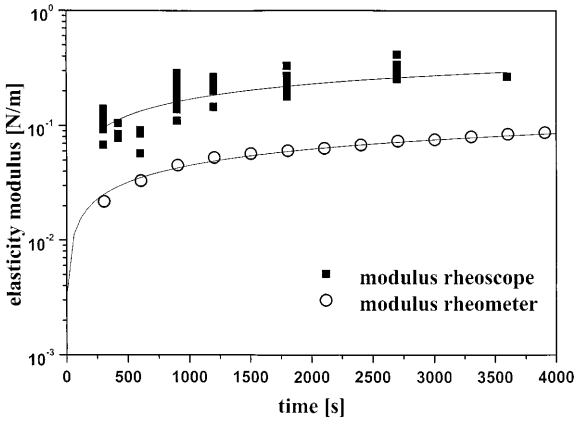

Fig. 9 Comparison of time-dependent E_s and G'

ization times from rheoscope measurements. These moduli, denoted as E_s, are plotted as a function of time in Fig. 9. We also measured the shear moduli as a function of the polymerization period and these values are also plotted in Fig. 9.

Both plots take a parallel course, indicating similar polymerization properties of curved and flat membranes. The discrepancy of a factor of 3–4 is in good agreement with a theoretical prediction recently proposed by Barthès-Biesel [15]. The discrepancy is caused by the fact that the elastic modulus measured with the rheoscope covers two modes of deformation (shear and dilatation), whereas the interfacial rheometer measures principally shear moduli.

A comparison of the two types of moduli obtained experimentally is only feasible by taking into account their different underlying constitutive laws. For the Mooney–Rivlin constitutive law, the shear modulus, E_{ss}^{MR}, is linked to the elastic modulus, E_s^{MR}, by the equation

$$E_{ss}^{MR} = \frac{E_s^{MR}}{3} \quad . \tag{9}$$

In case of pure shear and under the assumption of small deformations this shear modulus is equal to the shear modulus, E_{ss}^{H}, based on Hooke's law, which is measured by the rheometer. The values are related by the following expression:

$$\frac{E_s^{MR}}{3} = E_{ss}^{MR} = G' = E_{ss}^{H} \quad . \tag{10}$$

Consequently, the two moduli acquired experimentally are predicted to differ by about a factor of 3. In addition, it is important to note that the Hooke shear modulus correlates with the respective elastic modulus, E_s^H, according to

$$E_{ss}^{H} = \frac{E_s^{H}}{2(1+\nu_s)} \quad . \tag{11}$$

For a Mooney–Rivlin-type material, which is volume-incompressible, the Poisson ratio, ν_s, is 0.5, and using Eqs. (10) and (11) we obtain

$$E_{ss}^{MR} = \frac{E_s^{MR}}{2(1+0.5)} = \frac{E_s^{MR}}{3} \quad , \tag{12}$$

showing that in small deformations, the Mooney–Rivlin law is a restriction case of the more general Hooke constitutive law.

Conclusion

In this publication we have systematically compared results for flat and curved polyamide membranes at conditions of equal polymerization times. Both investigations are consistent and give complementary results. It turns out that the membranes are 1 order of magnitude more elastic than viscous. The elastic moduli relate to each other as predicted theoretically and thereby underscore the validity of the theory. We observe, in principle, the same relationship between the shear modulus and Young's modulus as was observed from previously performed spinning-drop experiments [13, 22]. Due to experimental restrictions like the onset of turbulence, capsule measurements could not be carried out up to rupture, but the ultimate stability of the cross-linked membranes was investigated by strain sweep experiments. The results show that the ultrathin films at the interface between oil and water can be deformed to a large extent before nonlinear effects or breaking processes occur. On close inspection one may also suppose that the elastic modulus, measured in the rheoscope, is not exactly equal to Young's modulus because it can also contain contributions from shearing processes. In order to test this assumption, we have started to compare this constant with experimental data obtained in the spinning-drop apparatus. This work is still in progress and we hope that these experiments will lead to more sophisticated theoretical models.

Acknowledgements Financial support of this work by grants from the "Deutsche Forschungsgemeinschaft" SFB 1690 and the "Fonds der Chemischen Industrie" is gratefully acknowledged. We benefited greatly from numerous discussions with D. Barthès-Biesel.

References

1. Fanger GO (1974) CHEMTECH 397
2. Barnes HA, Hutton JF, Walters K (1989) In: Walters K (ed) An Introduction to Rheology series, vol 3. Elsevier, Amsterdam, pp 13
3. Mathiowitz E, Cohen MD (1989) J Membr Sci 40:1
4. Mathiowitz E, Cohen MD (1989) J Membr Sci 40:27
5. Janssen LJJM, te Nijenhuis K (1992) J Membr Sci 65:59
6. Janssen LJJM, te Nijenhuis K (1992) J Membr Sci 65:69
7. Janssen LJJM, Boersma A, te Nijenhuis K (1993) J Membr Sci 79:11
8. Enkelmann V, Wegner G (1972) Makromol Chem 157:303
9. Enkelmann V, Wegner G (1975) Am Chem Soc Polym Prep 16:409
10. Jay AWL, Edwards MA (1968) Can J Physiol Pharmacol 46:731
11. Liu KK, Williams DR, Briscoe BJ (1996) Phys Rev E 54:6673
12. Chang KS, Olbricht WL (1993) J Fluid Mech 250:609
13. Pieper G, Rehage H, Barthès-Biesel D (1998) J Colloid Interface Sci 202:293
14. Burger A, Rehage H (1992) Angew Makromol Chem 202:31
15. Barthès-Biesel D (1998) Prog Colloid Polym Sci 111:58
16. Pozrikidis C (1995) J Fluid Mech 297:123
17. Chang KS, Olbricht WL (1993) J Fluid Mech 250:587
18. Chang TMS, McIntosh FC, Mason SG (1966) Can J Physiol Pharmacol 44:115
19. Barthès-Biesel D (1991) Physica A 172:103
20. Barthès-Biesel D, Sgaier H (1985) J Fluid Mech 160:119
21. Barthès-Biesel D (1980) J Fluid Mech 100:831
22. Rehage H, Achenbach B, Husmann H (1999) In: Stokke BT, Elgsaeter A (eds) Wiley Polymer Networks Group Review Series, vol 2. Wiley, New York, pp 443